Energy Storage and Conversion 2024, 2(3), 480.
https://doi.org/10.59400/esc.v2i3.480

Review

A mini review on electroosmotic phenomena in porous media

Yan Gao*, Chunling Wang, Zhuo Gong, Zhiqiang Li

College of Science, China Jiliang University, Hangzhou 310018, China
*** Corresponding author:** Yan Gao, P21080854007@cjlu.edu.cn

CITATION

Gao Y, Wang C, Gong Z, Li Z. A mini review on electroosmotic phenomena in porous media. Energy Storage and Conversion. 2024; 2(3): 480.
https://doi.org/10.59400/esc.v2i3.480

ARTICLE INFO

Received: 15 March 2024
Accepted: 29 June 2024
Available online: 10 July 2024

Abstract: The electroosmosis phenomenon in porous media finds widespread applications in various fields such as microfluidic systems, polymer electrolyte membrane fuel cells, oil and gas engineering, wastewater sludge dewatering, groundwater dynamics, etc. Therefore, the electroosmotic flow mechanism in porous media has attracted broad interest from multiple disciplines. This paper provides an overview of the physical mechanisms and mathematical models for electroosmosis in porous media. The background of electric double layer theory and state-of-the-art research progress on pore-scale models for electroosmotic flow through porous media are reviewed. Two typical and significant research topics, electroosmosis under pressure coupling effects and nanoscale electroosmotic phenomena, are then focused on. The advances in theoretical analysis, numerical simulation, and experimental measurements are summarized. Finally, the potential research directions for electroosmotic flow in porous media are addressed.

Keywords: electroosmosis; porous media; electric double layer; pressure coupling effect; nanoscale

1. Introduction

The electrokinetic phenomenon refers to the relative motion between solid and liquid phases or the generation of electric potential in colloidal systems where solid and liquid coexist under the influence of an applied electric field. Electrokinetic phenomena are generally classified into four categories [1]: electrophoresis, electroosmosis, streaming potential, and sedimentation potential. However, these four kinds of electrokinetic phenomena may coexist and have strong relationships with each other (as shown in **Figure 1**).

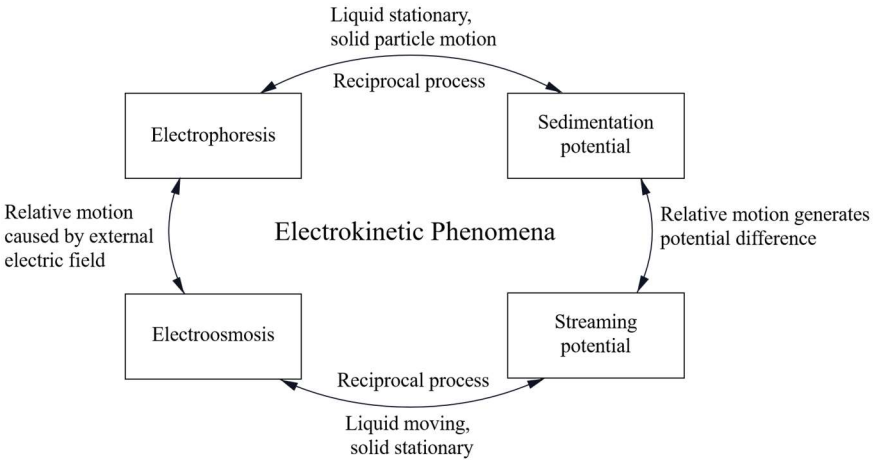

Figure 1. The relationship between electrokinetic phenomena.

In 1809, Russian scientist Ruess first observed the directed movement of clay particles under the influence of an electric field in experimental studies, which was termed electrophoresis [2]. And the solid clay particles may induce the movement of charged particles in the liquid phase, which is known as electroosmosis. Electroosmosis (also called electroosmotic flow, or EOF) can be considered the reverse process of electrophoresis. In 1852 and 1859, German physical chemists Wiedemann [3] and Quincke [4], respectively, found that when pressure is applied to a liquid passing through a porous ceramic plate, a potential difference is generated in the direction of flow. This phenomenon is called streaming potential. In 1878, German physicist Dorn [5] observed the settling of particles under the influence of gravity, resulting in a sedimentation potential. All of these phenomena mentioned above are collectively referred to as electrokinetic phenomena. Both the solid and liquid phases have charges on their surfaces, and the charges on the solid surface attract charges with equal magnitude but opposite polarity, forming an electric double layer (EDL) structure at the interface between the solid and liquid phases. The schematic diagram of electrokinetic phenomena is shown in **Figure 2**.

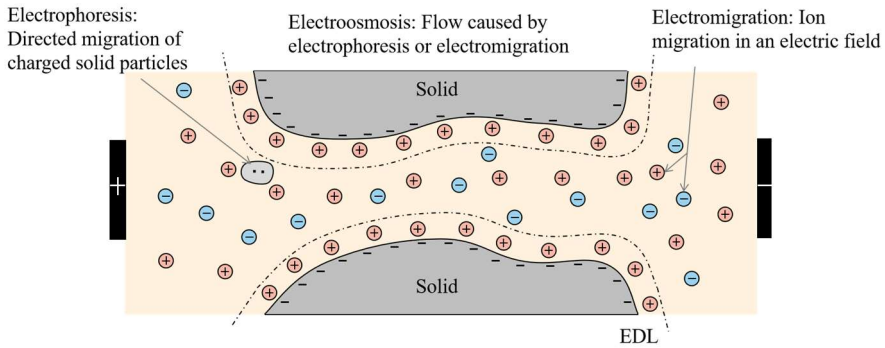

Figure 2. The schematic graph of electrokinetic phenomena.

Electrokinetic phenomena have been widely applied in various fields such as oil and gas engineering [6], energy and environmental technology [7], biomedical science [8], chemical industry [9], etc. In practical industrial applications, when an electric field acts on a charged fluid, the charged particles in the fluid are subjected to the force of the electric field, resulting in fluid flow. Studying this flow phenomenon is crucial for improving industrial production efficiency and reducing production costs, making in-depth research on the electroosmotic flow phenomenon of great significance. Electroosmotic flow is a key aspect of electrokinetic phenomena, describing the flow behavior of charged fluids at the microscale under the influence of an electric field. The application of electroosmotic flow covers a wide range of fields. For example, in the petroleum industry [10], the flow rate of oil can be increased by applying an external electric field, which enhances the oil recovery rate accordingly. In the field of microfluidic devices [11], lab-on-a-chip technology enables the miniaturization of sample preparation, reactions, separations, and detection techniques by using electrokinetic phenomena. In terms of cooling technology [12], the application of electrokinetic phenomena in microchannel cooling has potential for improving cooling performance. In sludge dewatering and treatment [13], the surface water can be effectively removed by electroosmosis. In the biomedical field, a minimally invasive

technique using a microneedle array combined with reverse iontophoresis has been employed to non-invasively extract interstitial fluid from the cellular interstitium below 25 millimeters from the skin surface. This technology enables more convenient medical devices for blood glucose monitoring [14] and drug delivery [15]. In the field of human-computer interaction, the development of tactile interaction devices utilizing electroosmotic pump arrays, such as tactile gloves [16], provides more immersive and realistic interactive experiences in virtual reality, augmented reality, and gaming. In the field of energy, electroosmotic flow is used for ion transport and mass separation in batteries, fuel cells, and supercapacitors [17].

Despite the significant progress made in electroosmosis research over the past few decades, there are still some drawbacks and limitations. The eletroosmosis phenomenon involves the coupling of multiple physical processes, such as the electric field, fluid mechanics, and electrolyte mass transfer. Current research often focuses on studying these processes separately, neglecting the interactions and coupling effects between them. And with the development of micro- and nanotechnology, the mechanisms of electroosmosis in nano-scale porous media are significant and attract broad interest. As a result, a comprehensive understanding of the electroosmotic flow behavior in complex and multiscale systems still requires further investigation. Therefore, this paper provides an overview of electrokinetic phenomena and an up-to-date review of eletroosmosis through porous media. The background and fundamentals of EDL are first introduced. And the pore-scale mathematical models of eletroosmosis through porous media are summarized and reviewed. Then, electroosmosis under pressure coupling effects and nanoscale electroosmotic mechanisms are explored. The research progress on theoretical analysis, numerical simulation, and experimental measurement in these two fields is presented. Finally, the possible and valuable research topics in electroosmosis through porous media are pointed out.

2. EOF in porous media

2.1. EDL theory

The EDL structure at the solid-liquid interface primarily discusses the distribution patterns of ions and the corresponding variations of potential with distance. Since the late 19th century, several physical models have been proposed to understand EDL and its mechanisms. In 1879, Helmholtz [18] first proposed a parallel plate model for EDL.

$$\sigma = \frac{\varepsilon_0 \varepsilon_r \psi_0}{\delta} \tag{1}$$

where σ represents the surface charge density of the solid, ε_r is the relative permittivity of the medium between the plates, ε_0 is the permittivity of vacuum, ψ_0 is the surface potential, and δ is the distance between the parallel plates. Between 1910 and 1913, Gouy [19] and Chapman [20] proposed a diffuse EDL model by introducing a diffuse layer into the Helmholtz model. That is, there are two electric layers at the charged interface in an electrolyte solution: the inner and outer layers (**Figure 3a**). This model is capable of characterizing the potential variation with distance from the plate. In 1924, Stern combined the Helmholtz model and the Gouy-Chapman model

to propose the Stern EDL model [21]. It consists of two parts: the stern layer and the diffuse layer. The layer adjacent to the surface is named the compact layer or Stern layer; the diffuse layer is between the Stern layer and the interior of the liquid phase. As shown in **Figure 3b**, the potentials of the solid phase and the Stern layer are ψ_0 and ψ_s, respectively. And δ and ξ denote the Stern layer thickness and potential at the diffuse layer boundary, respectively.

In order to study the EOF through porous media, the capillary model is generally employed to characterize the electroosmosis path. As shown in **Figure 4**, the potential at the capillary wall is denoted as ψ_0, the potential at a distance of r is denoted as $\psi(r)$, and the excess charge density is denoted as $\rho(r)$. By employing the Stern EDL model and considering a monovalent electrolyte, the Poisson equation becomes:

$$\frac{1}{r}\frac{d}{dr}\left[r\frac{d\psi(r)}{dr}\right] = -\frac{\rho(r)}{\varepsilon_r\varepsilon_0} \tag{2}$$

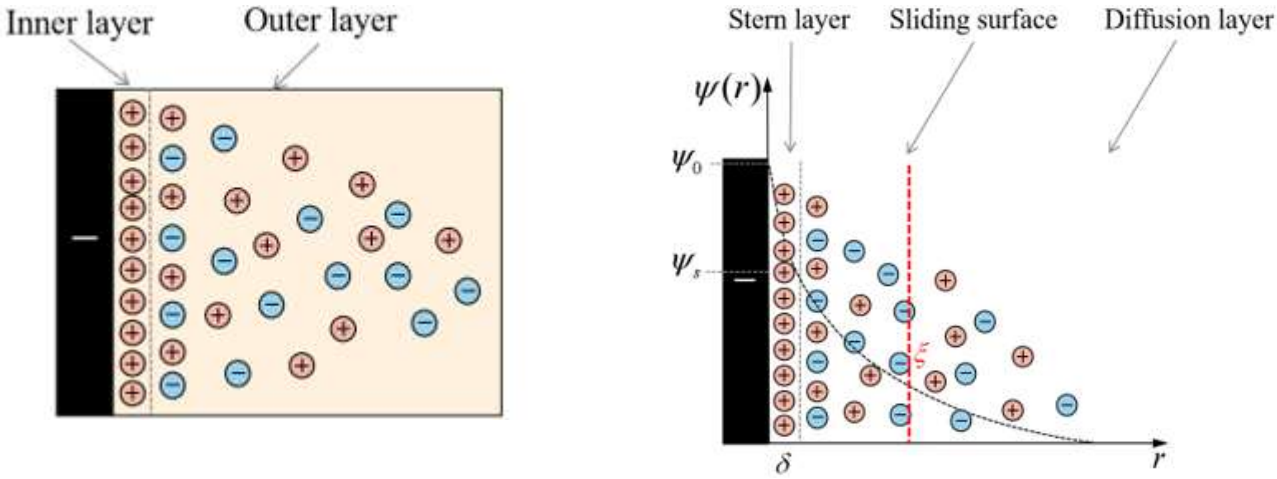

(a) Gouy-Chapman diffusion double layer model. **(b)** Stern double layer model.

Figure 3. Diffusion electric double-layer model.

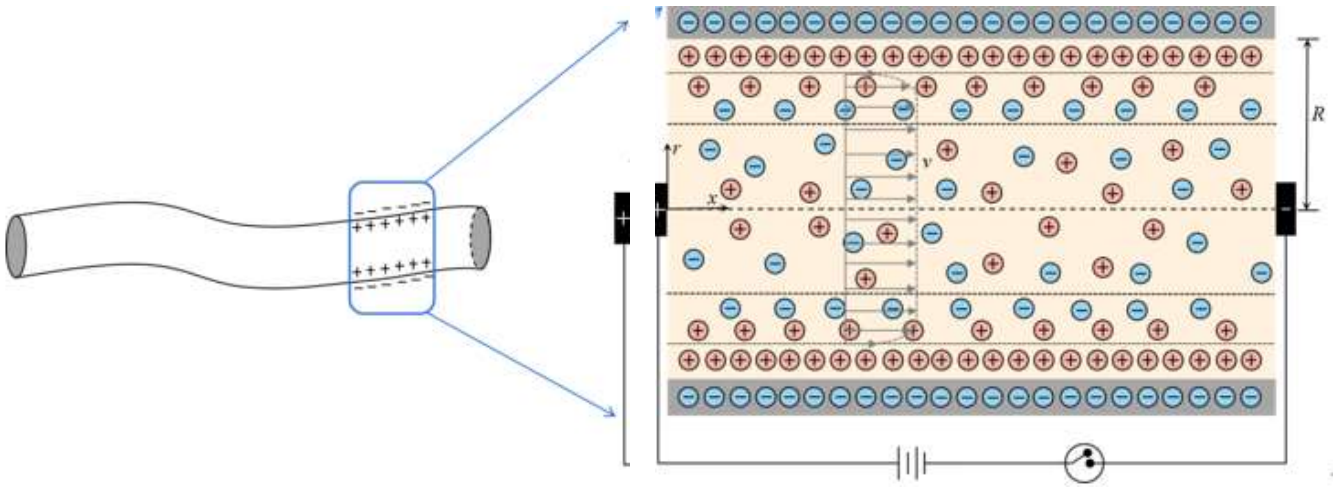

(a) Single capillary tube. **(b)** Electric double layer phenomenon in capillaries.

Figure 4. Schematic diagram of capillary double layer.

Based on Boltzmann equation, the charge density can be gotten as:

$$\rho(r) = -2ne\,sinh\frac{e\psi(r)}{kT} \tag{3}$$

where k is the Boltzmann's constant, T is temperature, n is the Avogadro number and e is the elementary charge. By using Debye–Hückel approximation, $\frac{e\psi(r)}{(kT)} \ll 1$ and $\frac{sinh\, e\psi(r)}{(kT)} \simeq \frac{e\psi(r)}{(kT)}$. It should be noted that this approximation would only be applicable to very small values of potential.

The Poisson-Boltzmann distribution equation then becomes

$$\frac{1}{r}\frac{d}{dr}\left[r\frac{d\psi(r)}{dr}\right] = \kappa^2\psi(r) \tag{4}$$

where $\kappa = \sqrt{\frac{2ne^2}{\varepsilon_0\varepsilon_r kT}}$ is the reciprocal of the EDL thickness. For a cylindrical capillary, the boundary conditions are as follows:

$$\psi(r) = \begin{cases} \left.\frac{d\psi(r)}{dr}\right|_{r=0} = 0 \\ \psi(R) = \psi_0 \end{cases} \tag{5}$$

Then, the analytical solutions for $\psi(r)$ and $\rho(r)$ are:

$$\psi(r) = \psi_0\frac{I_0(\kappa r)}{I_0(\kappa R)} \tag{6}$$

$$\rho(r) = -\varepsilon_0\varepsilon_r\kappa^2\psi_0\frac{I_0(\kappa r)}{I_0(\kappa R)} \tag{7}$$

where I_0 is the modified Bessel function of the first kind of zero order. The velocity profile $v(r)$ through a tortuous capillary under an electric field U can be expressed by:

$$v(r) = \frac{\varepsilon_0\varepsilon_r\psi_0 E}{\mu}\left[1 - \frac{I_0(\kappa r)}{I_0(\kappa R)}\right] \tag{8}$$

where μ is fluid viscosity, L_0 is the representative length of the porous media, $E=U/L_0$ is applied electric field gradient.

2.2. Progress on EOF

Porous media are composed of minerals (such as silicates, oxides, and carbonates) or other materials (such as polymers and biomaterials), and these porous materials typically carry charges due to isomorphic substitutions in their structure. In order to explore the EOF mechanism in porous media, theoretical analysis, numerical simulations, and experimental studies have been conducted on EOF in ideal and simplified devices, including capillaries, parallel plates, and microchannels. And the influences of device shape and size on EOF were investigated in detail.

In 1965, Rice and Whitehead [22] conducted a systematic theoretical analysis on electrokinetic phenomena in narrow cylindrical capillaries using the Debye-Hückel approximation, which is only applicable in small surface potential. Later, Levine et al. [23] and Olivares et al. [24] extended the theory proposed by Rice and Whitehead by dividing the capillary into low surface potential regions and high surface potential regions and solving for the surface potential in each region. In 1990, Ohshima and Kondo [25] derived simple approximate analytical formulas for electroosmotic velocity, volume flow rate, current, and streaming potential in the study of the electrokinetic effect between two parallel plates. In 1997, Mala et al. [26] explored the influence of the electrokinetic effect on the liquid flow characteristics in

microchannels between two parallel plates. In 2013, Luong and Sprik [27] conducted U-tube experiments in saturated porous media to measure the relationship between the electrokinetic effect and electric field strength, aiming to assess the permeability and pore structure of the material. In 2020, Luo and Keh [28] analyzed the electrokinetic flow and accompanying electrical conduction of salt-free solutions in charged circular capillaries along the axial direction. They solved for the electrostatic potential distribution and fluid velocity distribution within the capillary channel. In 2022, Ning et al. [29] utilized a fractal capillary bundle model to develop the electro-hydrodynamic coupling process in non-steady pressure-driven flows. They derived analytical expressions for the potential distribution and velocity distribution within the channels.

Capillary models with different geometries have been proposed to study EOF in porous media. For example, Paillat et al. [30] studied the EOF in porous media based on a single capillary; Wu and Papadopoulos [31] used cylindrical and annular capillary bundle models to study the EOF in porous media; and Pascal et al. [32] examined the impact of rectangular, cylindrical, and annular ideal capillaries on the EOF flow rate in porous fibrous media. Since the pore structures of porous media indicate random and irregular characteristics, fractal geometry has been proposed to develop a pore-scale model for EOF in porous media. In 2013, Bandopadhyay et al. [33] used fractal theory to study EOF characteristics in porous media with irregular or non-uniform terrain features, investigated the influence of the conductivity tensor on domain morphology and solid fraction, and compared it with the equivalent Darcy permeability. In 2015, Liang et al. [34] analyzed the electroosmotic characteristics in fractal porous media and investigated the factors that influence the height difference. In 2020, Thanh et al. [35] obtained theoretical expressions for the electroosmotic pressure coefficient and permeability of porous media based on a tortuous fractal cylindrical capillary bundle model. In 2023, Xu et al. [36] established a new pore-scale physical model for EOF in sludge porous media and derived the analytical expressions for EOF flow rate and permeability.

The external electric field or pressure has been proposed on the microchannel walls to modulate the electroosmotic effect and thereby control the fluid velocity and flow distribution. In 2011, Vennela et al. [37] studied the Sherwood number due to the combined flow driven by pressure and electroosmotic flow in porous microtubes. In 2013, Dutta [38] theoretically investigated the electroosmotic flow characteristics of nanofluidic separation of non-neutral analytes by combining the forward pressure gradient with the counteracting force electroosmotic flow field. In 2019, Kou and Dejam [39] studied the dispersion phenomena caused by pressure and electroosmotic flow in channels surrounded by permeable porous media. In 2019, Rosenfeld and Bercovici [40] employed an electroosmotic pump to control capillary flow, where the applied voltage could regulate the capillary driving speed. They investigated the filling, mixing, and transport of liquids in a microfluidic paper-based analytical device. In 2020, Godinez-Brizuela and Niasar [41] mainly investigated the flow generated by the simultaneous action of pressure and electroosmotic flow in charged porous media and studied the pore-scale effects in mixing and dispersion processes. In 2024, Terutsuki et al. [42] utilized the electroosmotic flow generated by the combination of anion and cation hydrogels to achieve electroosmotic flow-controlled delivery,

thereby realizing chemical transport. In 2024, Mondal and Chaube [43] investigated the peristaltic flow of unstable, viscous, and incompressible fluids in capillary channels under two-dimensional conditions. They simplified the model and derived analytical expressions for the electroosmotic characteristics, considering the thin EDL situation.

3. EOF with pressure effect

Both pressure-driven and electroosmosis-driven flow are important methods for fluid propulsion. Compared with common pressure-driven flow, electroosmosis-driven flow offers advantages such as low cost, high efficiency, a long lifespan, ease of operation and control, etc. The pressure-driven flow generally forms a parabolic velocity profile (**Figure 5a**), while the electroosmosis-driven flow exhibits a plug-like flow profile (**Figure 5b**). The uniform velocity distribution across the cross-section enables the precise separation of samples by electrophoresis.

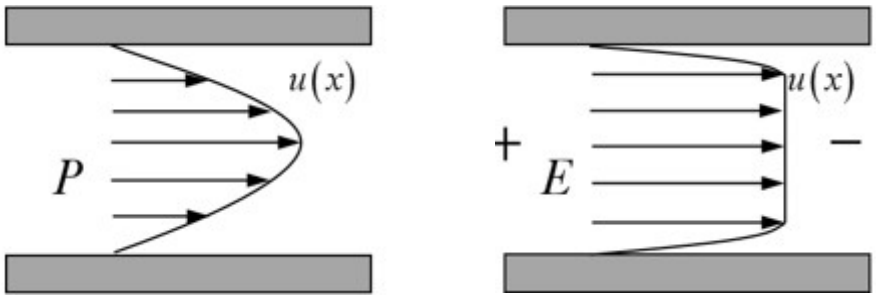

(a) Pressure-driven velocity profile. **(b)** Electroosmosis-driven velocity profile.

Figure 5. Velocity profile of pressure-driven and Electroosmosis-driven flow.

When considering the pressure effect in electroosmotic flow, the choice of an appropriate model depends on the specific conditions and requirements of the system. Two commonly used models for incorporating the pressure effect in electroosmotic flow are the Helmholtz-Smoluchowski (HS) model and the Modified Helmholtz-Smoluchowski (MHS) model. The HS model is only suitable for low-pressure systems. While the effect of fluid compressibility is included in the MHS model.

The flow rate of EOF with pressure effect depends on the applied electric field, zeta potential of the channel walls, fluid properties (viscosity, conductivity), channel geometry, pressure gradient, and even the presence of additional external forces. Various empirical or semi-empirical equations have been proposed to describe the EOF flow with pressure, that is, simultaneous pressure and electroosmosis-driven flow. As illustrated in **Table 1**, there is a clear difference between these available models for flow rate. Rice and Whitehead [22] proposed a narrow, straight cylindrical capillary model based on the double-layer theory and Boltzmann equation. They derived the electroosmotic flow velocity and electroosmotic flow rate and discussed the relationship between electroosmotic phenomena and flow radius. Kobayashi et al. [44] designed a vertical electroosmotic experimental setup, considering factors such as gravity, pressure, and electric field forces. They got the potential distribution, electroosmotic flow velocity, and electroosmotic flow rate in capillary channels. Paillat et al. [30] used a cylindrical straight capillary model, the pore radius of which

is much larger than the EDL thickness, to derive the electroosmotic flow velocity. Vennela et al. [37] used a two-dimensional cylindrical micro-pore model based on the EDL theory and the Boltzmann equation and explored the relationship between the Sherwood number and the Debye length. Dutta [38] carried out a numerical simulation on a two-parallel-plate channel model to investigate the charge separation in nanofluids. They derived a normalized electroosmotic flow velocity equation. Thanh et al. [35] utilized a curved cylindrical channel model based on fractal theory and obtained electroosmotic flow velocity and electroosmotic flow rate inside the channel.

The pressure-driven flow through a cylindrical and tortuous capillary with a radius of R can be characterized by the Hagen-Poiseuille equation. Thus, according to Equation (8) under the Debye-Hückel approximation, the flow velocity under the simultaneous effect of pressure and electric field can be written as:

$$v(r) = -\frac{1}{4\mu}(R^2 - r^2)\frac{\Delta P}{L_\tau} + \frac{\varepsilon_0 \varepsilon_r |\zeta| E}{\mu}\left[1 - \frac{I_0(\kappa r)}{I_0(\kappa R)}\right] \tag{9}$$

Therefore, the volumetric flow rate in the capillary is given by:

$$q(R) = \int_0^R v(r)\, 2\pi r dr = -\frac{\pi R^4}{8\mu}\frac{\Delta P}{L_\tau} + \frac{\pi \varepsilon_0 \varepsilon_r |\zeta| R^2 E}{\mu}\left[1 - \frac{2I_1(\kappa R)}{\kappa R I_0(\kappa R)}\right] \tag{10}$$

where I_1 is the first-order modified Bessel function of the first kind.

Figure 6 illustrates the variation of $C = 1 - \frac{2I_1(\kappa R)}{[\kappa R I_0(\kappa R)]}$ with the radius R. It can be observed that as the radius R of the capillary increases, the value of C approaches to 1. Therefore, the flow rate in a single capillary under simultaneous effect of pressure and electric field can be simplified as:

$$q(R) = -\frac{\pi R^4}{8\mu}\frac{\Delta P}{L_\tau} + \frac{\pi \varepsilon_0 \varepsilon_r |\zeta| R^2 E}{\mu} \tag{11}$$

Table 1. Flow rate of EOF with pressure effect.

Flow rate	Geometric model	References
$v(r) = \frac{P}{4\mu}(a^2 - r^2) - \frac{\varepsilon\zeta}{4\pi\mu}E\left[1 - \frac{I_0(\kappa r)}{I_0(\kappa a)}\right]$	narrow straight cylindrical capillary model	[20]
$v(r) = \frac{\varepsilon\zeta E_z}{\mu}\left(\frac{I_0(\kappa a)}{I_0\{\kappa(d/2-\delta)\}} - 1\right) + \frac{(d/2-\delta)^2 - a^2}{4\mu}\left(-\frac{dP}{dz}\right)$	vertical straight cylindrical capillary model	[39]
$v(r) = \frac{\Delta P}{4\mu L}(r^2 - a^2) - E\rho_p\delta_0^2\left[\frac{I_0(r/\delta) - I_0(a/\delta_0)}{I_0(a/\delta_0)}\right]$	cylindrical straight capillary model	[28]
$v(r) = \frac{a^2 P}{4\mu}\left[1 - \left(\frac{r}{a}\right)^2\right] - \frac{\varepsilon\zeta E_x}{\mu}\left[1 - \frac{I_0(\kappa r)}{I_0(\kappa a)}\right]$	two-dimensional cylindrical micro-pore model	[35]
$v^*(r) = \frac{3}{2}(1 + ff\left\{\frac{1 - cosh(\kappa y^*)/cosh(\kappa/2)}{1 - tanh(\kappa y^*)/(\kappa/2)}\right\}$	two-parallel-plate channel model	[36]
$v(r) = -\frac{1}{4\mu}(a^2 - r^2)\frac{\Delta P}{L_\tau} + \frac{\varepsilon_0\varepsilon_r\zeta}{\mu}\left[1 - \frac{I_0(\kappa r)}{I_0(\kappa a)}\right]\frac{\Delta V}{L}$	curved cylindrical channel model	[33]

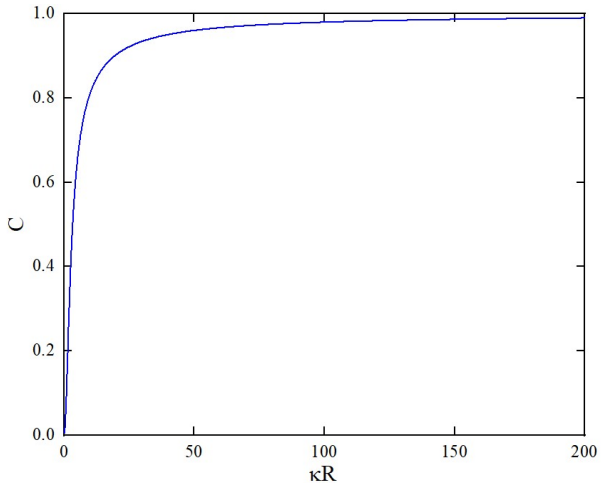

Figure 6. Variation of the dimensionless coefficient C with the dimensionless ratio of pore size to Debye length.

4. EOF in nano porous media

Most of the available research was performed on the EOF in porous media with a regular pore size, where the thickness of the EDL can be neglected. However, the electroosmotic phenomenon in porous media with micro- to nanoscale pores is greatly influenced by the EDL because the thickness of the EDL is comparable to the radius of the capillary, and the EDL poses a certain hindrance to fluid flow. The classical Poisson-Boltzmann equation cannot accurately describe the particle distribution inside micro-nano channels/pores, especially in the region close to the solid phase. This is mainly due to the fact that the interactions between ion-ion and solid wall atom-ion are neglected in the continuum theoretical models, which become significant at the nanoscale. Therefore, the EOF in nanoscale porous media brings new challenges and attracts broad interests.

In order to measure the velocity distribution, concentration distribution, and flow patterns inside micro- and nano-scale channels and pores, a few experimental techniques were proposed and applied (as shown in **Table 2**). So far, visualization experiments can be broadly categorized into trajectory line methods [45], bright field observation methods [46], micro-PIV particle velocimetry methods [47], LIF (laser-induced fluorescence) methods [48], and chromatography techniques [49]. The trajectory line method, also known as trajectory analysis, involves tracking the movement path and velocity of tracer particles to obtain the fluid's flow trajectories and velocity distribution. The bright field observation method utilizes high-speed cameras or microscopes to directly observe the flow behavior inside channels or pores, capturing real-time flow images for studying fluid flow and separation phenomena. The Micro-PIV (Particle Image Velocimetry) particle velocity measurement method employs laser illumination and high-speed imaging technology to track the positions of tracer particles at different time intervals, thereby obtaining information about the fluid velocity field and other parameters. Laser-Induced Fluorescence (LIF) utilizes laser illumination to excite fluorescent tracers in the fluid, capturing the signals with a camera or spectrometer to obtain information about fluid concentration distribution and particle transport. Chromatography techniques are employed to study the

separation and diffusion of fluids in channels or pores. By measuring the degree of separation and transfer rates, information about fluid concentration distribution and separation efficiency can be obtained. These visualization experimental techniques provide quantitative analysis of flow behavior inside micro- and nano-scale channels and pores. By combining these experimental techniques, researchers can investigate the physical mechanisms of fluids at the microscale and establish related mathematical models.

Table 2. The visualization experimental methods for nanoscale EOF.

Types	Characteristic	Parameter	References
Trajectory Line Method	Contact measurement, direct and simple, lower accuracy, two-dimensional field measurement	streamline, velocity	[45]
Bright-field Observation Method	Non-contact measurement, direct observation, simple structure	flow pattern, velocity	[50]
Micro Particle Image Velocity	Non-contact measurement, high accuracy, capable of measuring both planar and three-dimensional velocity fields	velocity vectors, flow field distribution, concentration	[51]
Laser Induced Fluorescence	Non-contact measurement, high precision and resolution	velocity vectors, flow pattern, concentration, temperature	[52]
Chromatography technology	Non-contact measurement, two-dimensional field measurement	Two-dimensional flow field	[49]

With the rapid development of computer technology, simulation methods including molecular dynamics simulation (MD), Monte Carlo simulation (MC), Brownian dynamics simulation (BD), and dissipative particle dynamics simulation (DPD) have been frequently adopted to study and understand EOF mechanisms in nanoscale porous media.

The MD utilizes Newton's equations of motion to numerically solve the classical mechanics equations for molecular systems, obtaining the system's trajectory and calculating its structural characteristics and properties. This method is known for its high accuracy in computational results. Marx and Hutter [53] provided a detailed introduction to ab initio MD, including the fundamental theory, electronic structure calculations, and simulation techniques. Kim and Darve [54] investigated EOF in charged nanoscale channels with different surface roughness using equilibrium and non-equilibrium MD. Zhang et al. [55] developed a three-dimensional MD model for EOF in rough nanoscale channels to explore the influence of surface roughness on nanoscale EOF. Rezaei et al. [56] studied the EOF of an aqueous solution between parallel silicon walls using MD, considering the effects of changes in the EDL structure characteristics. Gogoi et al. [57] discussed in detail the EOF characteristics of rectangular graphene nanoscale channels with different charge configurations using non-equilibrium MD. Dehkordi et al. [58] investigated the effect of external electrostatic forces and external electric fields on the density, velocity, atomic structure, temperature, and agglomeration of Fe_3O_4 nanoparticles in copper microchannels using MD.

The MC method is a numerical computation method guided by probability and statistical theory. It has been proposed in computational simulation for discrete systems. Freund [59] conducted atomic simulations of EOF in nanoscale channels using MC to study ion distributions. Lee et al. [60] numerically investigated the effect

of alternating current EOF on the performance of a biosensor unit composed of 400 nanometer wires using the MC method. Xin et al. [61], based on the improved fundamental measure theory and partial perturbation density functional theory, studied the distribution and density of ions in charged cylindrical pores with MC.

The BD can be used to simulate molecular motion and interactions, where molecules are treated as moving in a continuous medium and subject to various forces such as van der Waals forces, electrostatic forces, and solvent molecule forces. Marry et al. [62] obtained the distribution of counterions in mesoscale charged porous media using BD and Poisson-Boltzmann. Panwar and Kumar [63] employed BD to study the stretching and transport of flexible polymers in complex EOF.

The DPD is a mesoscale particle-based simulation algorithm, where a particle represents a group of atoms retaining important chemical characteristics in order to simulate the system with fewer particles instead of individual atoms. Using DPD, Duong [64] proposed a mesoscale method to describe EOF in micro/nanofluidic devices that were too large to be simulated using ab initio methods. Moshfegh and Jabbarzadeh [65] conducted explicit mesoscale simulations of EOF in nanoscale channels using an extended DPD approach. Smiatek and Schmid [66], who used DPD to simulate EOF in nanoscale channels under different surface slip conditions and ion-strength fluids, introduced appropriately tuned wall-fluid friction to systematically adjust the slip length at the channel boundaries from negative to infinitely large values.

5. Concluding remarks

EOF in porous media is an important physical phenomenon with wide-ranging potential applications in various fields. This mini-review provides an overview of the physical mechanisms and mathematical models of EOF in porous media. Up-to-date progress on EOF mechanisms in porous media has been summarized. And two subtopics, simultaneous pressure and electroosmosis-driven flow and nanoscale EOF, have been explored. The advances in these two subfields are reviewed. The present review helps understand the complex EOF mechanisms and explore potential applications of EOF in engineering and industry.

Based on the present review, the following topics may be future research directions: (1) The unique EOF properties of novel porous materials can be explored for potential applications in energy, the environment, biomedical fields, etc. (2) Attention can be directed towards the coupling of electroosmosis with other physical phenomena such as electrochemical reactions, heat conduction, and mass transfer. These multiphysical fields may help explore the role of EOF in broader domains, such as battery technology, electrochemical sensors, and microfluidic control. (3) As illustrated in this paper, EOF mechanisms for microscale and mesoscale porous media have attracted broad interest. A few mathematical models have been proposed. However, multiscale EOF phenomena may coexist in multiscale porous media where multiple physical mechanisms govern EOF. Therefore, it is necessary to develop physical models and numerical methods applicable to different scales, thereby bridging the microscopic EOF with macroscopic system performance.

Conflict of interest: The authors declare no conflict of interest.

References

1. Delgado AV, González-Caballero F, Hunter RJ, et al. Measurement and interpretation of electrokinetic phenomena. Journal of Colloid and Interface Science. 2007; 309(2): 194-224. doi: 10.1016/j.jcis.2006.12.075
2. Reuss FF. On a new effect of galvanic electricity (French). Soc. Imp. Natur. Moscou. 1809; 2: 327-337.
3. Wiedemann M. On the motion of fluids from the positive to the negative pole of the closed galvanic circuit. The London, Edinburgh, and Dublin Philosophical Magazine and Journal of Science. 1852; 4(28): 546-547. doi: 10.1080/14786445208647182
4. Quincke G. About a new type of electric current (German). Annalen der Physik. 1859; 183(5): 1-47. doi: 10.1002/andp.18591830502
5. Dorn E. On the propagation of electricity through flowing water in pipes and related phenomena (German). Annalen der Physik. 1880; 246(5): 46-77. doi: 10.1002/andp.18802460505
6. Saunders JH, Jackson MD, Pain CC. Fluid flow monitoring in oil fields using downhole measurements of electrokinetic potential. Geophysics. 2008; 73(5): E165-E180. doi: 10.1190/1.2959139
7. Millán M, Bucio-Rodríguez PY, Lobato J, et al. Strategies for powering electrokinetic soil remediation: A way to optimize performance of the environmental technology. Journal of Environmental Management. 2020; 267: 110665. doi: 10.1016/j.jenvman.2020.110665
8. Dehghan Manshadi MK, Khojasteh D, Mohammadi M, et al. Electroosmotic micropump for lab-on-a-chip biomedical applications. International Journal of Numerical Modelling: Electronic Networks, Devices and Fields. 2016; 29(5): 845-858. doi: 10.1002/jnm.2149
9. Grassia P. Viscous and electro-osmotic effects upon motion of an oil droplet through a capillary. Journal of Fluid Mechanics. 2020; 899. doi: 10.1017/jfm.2020.458
10. Yang S, Zhang H, Hu Y, et al. Experimental study on remediation of petroleum-contaminated soil by combination of freeze-thaw and electro-osmosis. Environmental Pollution. 2023; 333: 121989. doi: 10.1016/j.envpol.2023.121989
11. Jiang S, Zhang H, Chen L, et al. Numerical simulation and experimental study of the electroosmotic flow in open microfluidic chip based on super-wettability surface. Colloid and Interface Science Communications. 2021; 45: 100516. doi: 10.1016/j.colcom.2021.100516
12. Pramod K, Sen AK. Flow and Heat Transfer Analysis of an Electro-Osmotic Flow Micropump for Chip Cooling. Journal of Electronic Packaging. 2014; 136(3). doi: 10.1115/1.4027657
13. Xu H, Ding T. Influence of vacuum pressure, pH, and potential gradient on the vacuum electro-osmosis dewatering of drinking water treatment sludge. Drying Technology. 2016; 34(9): 1107-1117. doi: 10.1080/07373937.2015.1095203
14. Zhang R, Miao Q, Deng D, et al. Research progress of advanced microneedle drug delivery system and its application in biomedicine. Colloids and Surfaces B: Biointerfaces. 2023; 226: 113302. doi: 10.1016/j.colsurfb.2023.113302
15. He Q, Zhao J, Du S, et al. Reverse iontophoresis generated by porous microneedles produces an electroosmotic flow for glucose determination. Talanta. 2024; 267: 125156. doi: 10.1016/j.talanta.2023.125156
16. Shen V, Rae-Grant T, Mullenbach J, et al. Fluid Reality: High-Resolution, Untethered Haptic Gloves using Electroosmotic Pump Arrays. In: Proceedings of the 36th Annual ACM Symposium on User Interface Software and Technology; 29 October-1 November 2023; San Francisco, CA, USA. pp. 1-20. doi: 10.1145/3586183.3606771
17. Yuan Y, Abdullah MM, Sajadi SM, et al. Numerical investigation of the effect of changing the geometry of a U-shaped fuel cell channel with asymmetric gas flow and its effect on hydrogen consumption. International Journal of Hydrogen Energy. 2024; 50: 1167-1178. doi: 10.1016/j.ijhydene.2023.10.080
18. Helmholtz H. Studies on electrical interfaces (German). Annalen der Physik. 1879; 243(7): 337-382. doi: 10.1002/andp.18792430702
19. Gouy G. On the Formation of Electrical Charges at the Surface of an Electrolyte. J. physique. 1910; 9: 457-469.
20. Chapman DL. LI. A contribution to the theory of electrocapillarity. The London, Edinburgh, and Dublin Philosophical Magazine and Journal of Science. 1913; 25(148): 475-481. doi: 10.1080/14786440408634187
21. Stern A. On the counter-transference in psychoanalysis. The Psychoanalytic Review (1913-1957). 1924; 11: 166.
22. Rice CL, Whitehead R. Electrokinetic Flow in a Narrow Cylindrical Capillary. The Journal of Physical Chemistry. 1965; 69(11): 4017-4024. doi: 10.1021/j100895a062
23. Levine S, Marriott J R, Neale G, et al. Theory of electrokinetic flow in fine cylindrical capillaries at high zeta-potentials.

Journal of Colloid and Interface Science. 1975; 52(1): 136-149. doi: 10.1016/0021-9797(75)90310-0
24. Olivares J, Casadesus J, Bedmar EJ. Method for Testing Degree of Infectivity of Rhizobium meliloti Strains. Applied and Environmental Microbiology. 1980; 39(5): 967-970. doi: 10.1128/aem.39.5.967-970.1980
25. Ohshima H, Kondo T. Electrokinetic flow between two parallel plates with surface charge layers: Electro-osmosis and streaming potential. Journal of colloid and interface science. 1990; 135(2): 443-448. doi: 10.1016/0021-9797(90)90014-f
26. Mala G M, Li D, Werner C, et al. Flow characteristics of water through a microchannel between two parallel plates with electrokinetic effects. International journal of heat and fluid flow. 1997; 18(5): 489-496. doi: 10.1016/s0142-727x(97)00032-5
27. Luong DT, Sprik R. Streaming Potential and Electroosmosis Measurements to Characterize Porous Materials. ISRN Geophysics. 2013; 2013: 1-8. doi: 10.1155/2013/496352
28. Luo RH, Keh HJ. Electrokinetic flow and electric conduction of salt-free solutions in a capillary. Electrophoresis. 2020; 41(16-17): 1503-1508. doi: 10.1002/elps.202000052
29. Ning K, Wang M, Kulacki FA, et al. Electrokinetic coupling in unsteady pressure-driven flow through a porous transducer: Fractal capillary bundle model. International Journal of Heat and Mass Transfer. 2022; 195: 122764. doi: 10.1016/j.ijheatmasstransfer.2022.122764
30. Paillat T, Moreau E, Grimaud PO, et al. Electrokinetic phenomena in porous media applied to soil decontamination. IEEE Transactions on Dielectrics and Electrical Insulation. 2000; 7(5): 693-704. doi: 10.1109/94.879363
31. Wu RC, Papadopoulos KD. Electroosmotic flow through porous media: cylindrical and annular models. Colloids and Surfaces A: Physicochemical and Engineering Aspects. 2000; 161(3): 469-476. doi: 10.1016/s0927-7757(99)00209-5
32. Pascal J, Oyanader M, Arce P. Effect of capillary geometry on predicting electroosmotic volumetric flowrates in porous or fibrous media. Journal of Colloid and Interface Science. 2012; 378(1): 241-250. doi: 10.1016/j.jcis.2012.03.061
33. Bandopadhyay A, DasGupta D, Mitra SK, et al. Electro-osmotic flows through topographically complicated porous media: Role of electropermeability tensor. Physical Review E. 2013; 87(3). doi: 10.1103/physreve.87.033006
34. Liang M, Yang S, Miao T, et al. Analysis of electroosmotic characters in fractal porous media. Chemical Engineering Science. 2015; 127: 202-209. doi: 10.1016/j.ces.2015.01.030
35. Thanh LD, Jougnot D, Van Do P, et al. Electroosmotic Coupling in Porous Media, a New Model Based on a Fractal Upscaling Procedure. Transport in Porous Media. 2020; 134(1): 249-274. doi: 10.1007/s11242-020-01444-7
36. Xu C, Xu Y, Wang J, et al. A Pore-Scale Physical Model for Electric Dewatering of Municipal Sludge Based on Fractal Geometry. Journal of Environmental Engineering. 2023; 149(3). doi: 10.1061/joeedu.eeeng-7089
37. Vennela N, Bhattacharjee S, De S. Sherwood number in porous microtube due to combined pressure and electroosmotically driven flow. Chemical Engineering Science. 2011; 66(24): 6515-6524. doi: 10.1016/j.ces.2011.09.016
38. Dutta D. A numerical analysis of nanofluidic charge based separations using a combination of electrokinetic and hydrodynamic flows. Chemical Engineering Science. 2013; 93: 124-130. doi: 10.1016/j.ces.2013.01.062
39. Kou Z, Dejam M. Dispersion due to combined pressure-driven and electro-osmotic flows in a channel surrounded by a permeable porous medium. Physics of Fluids. 2019; 31(5): 056603. doi: 10.1063/1.5092199
40. Rosenfeld T, Bercovici M. Dynamic control of capillary flow in porous media by electroosmotic pumping. Lab on a Chip. 2019; 19(2): 328-334. doi: 10.1039/c8lc01077c
41. Godinez-Brizuela OE, Niasar VJ. Simultaneous pressure and electro-osmosis driven flow in charged porous media: Pore-scale effects on mixing and dispersion. Journal of Colloid and Interface Science. 2020; 561: 162-172. doi: 10.1016/j.jcis.2019.11.084
42. Terutsuki D, Miyazawa S, Takagi J, et al. Spatiotemporally Controllable Chemical Delivery Utilizing Electroosmotic Flow Generated in Combination of Anionic and Cationic Hydrogels. Advanced Functional Materials. 2023; 34(2). doi: 10.1002/adfm.202304946
43. Mondal D, Chaube M K. Study on Electroosmotic Transport of Peristaltic Flow in Microchannel. 2024; 13(1). doi:10.9790/1813-13013543
44. Kobayashi K, Iwata M, Hosoda Y, et al. Fundamental study of electroosmotic flow through perforated membrane. Journal of Chemical Engineering of Japan.1979; 12(6): 466-471. doi: 10.1252/jcej.12.466
45. Kroger T, Tomiczek A, Wahl F. Towards On-Line Trajectory Computation. In: Proceedings of the 2006 IEEE/RSJ International Conference on Intelligent Robots and Systems; 9-15 October 2006; Beijing, China. pp. 736-741. doi: 10.1109/iros.2006.282622

46. Maksimenko A, Ando M, Sugiyama H, et al. A Test of an X-Ray Quatrochrome Interferometer for Simultaneous Observation of Images Due to Dark- and Bright-Field, Phase-Interference and Absorption Contrasts. Japanese Journal of Applied Physics. 2003; 42(Part 2, No.9A/B): L1096-L1099. doi: 10.1143/jjap.42.l1096
47. Lindken R, Rossi M, Große S, et al. Micro-Particle Image Velocimetry (μPIV): Recent developments, applications, and guidelines. Lab on a Chip. 2009; 9(17): 2551. doi: 10.1039/b906558j
48. Van de Nesse RJ, Velthorst NH, Brinkman UAT, et al. Laser-induced fluorescence detection of native-fluorescent analytes in column liquid chromatography, a critical evaluation. Journal of Chromatography A. 1995; 704(1): 1-25. doi: 10.1016/0021-9673(95)00053-p
49. Šesták J, Moravcová D, Kahle V. Instrument platforms for nano liquid chromatography. Journal of Chromatography A. 2015; 1421: 2-17. doi: 10.1016/j.chroma.2015.07.090
50. Chen J, Li H, Xie H, et al. A novel method combining aptamer-Ag10NPs based microfluidic biochip with bright field imaging for detection of KPC-2-expressing bacteria. Analytica Chimica Acta. 2020; 1132: 20-27. doi: 10.1016/j.aca.2020.07.061
51. Wereley ST, Meinhart CD. Recent Advances in Micro-Particle Image Velocimetry. Annual Review of Fluid Mechanics. 2010; 42(1): 557-576. doi: 10.1146/annurev-fluid-121108-145427
52. Murniati E, Gross D, Herlina H, et al. Oxygen imaging at the sediment-water interface using lifetime-based laser induced fluorescence (τLIF) of nano-sized particles. Limnology and Oceanography: Methods. 2016; 14(8): 506-517. doi: 10.1002/lom3.10108
53. Marx D, Hutter J. Ab initio molecular dynamics: Theory and implementation. Modern methods and algorithms of quantum chemistry. 2000; 1(301-449): 141.
54. Kim D, Darve E. Molecular dynamics simulation of electro-osmotic flows in rough wall nanochannels. Physical Review E. 2006; 73(5). doi: 10.1103/physreve.73.051203
55. Zhang C, Lu P, Chen Y. Molecular dynamics simulation of electroosmotic flow in rough nanochannels. International Communications in Heat and Mass Transfer. 2014; 59: 101-105. doi: 10.1016/j.icheatmasstransfer.2014.10.024
56. Rezaei M, Azimian AR, Semiromi DT. The surface charge density effect on the electro-osmotic flow in a nanochannel: a molecular dynamics study. Heat and Mass Transfer. 2014; 51(5): 661-670. doi: 10.1007/s00231-014-1441-y
57. Gogoi A, Reddy KA, Mondal PK. Electro-osmotic flow through nanochannel with different surface charge configurations: A molecular dynamics simulation study. Physics of Fluids. 2021; 33(9). doi: 10.1063/5.0062031
58. Dehkordi RB, Toghraie D, Hashemian M, et al. The effects of external force and electrical field on the agglomeration of Fe_3O_4 nanoparticles in electroosmotic flows in microchannels using molecular dynamics simulation. International Communications in Heat and Mass Transfer. 2021; 122: 105182. doi: 10.1016/j.icheatmasstransfer.2021.105182
59. Freund JB. Electro-osmosis in a nanometer-scale channel studied by atomistic simulation. The Journal of Chemical Physics. 2002; 116(5): 2194-2200. doi: 10.1063/1.1431543
60. Lee CA, Teramoto A, Watanabe H. Monte Carlo Simulation of Nanowires Array Biosensor with AC Electroosmosis. IEEE Transactions on Electron Devices. 2018; 65(5): 1932-1938. doi: 10.1109/ted.2018.2812783
61. Xin Y, Zheng YX, Yu YX. Density functional theory study on ion adsorption and electroosmotic flow in a membrane with charged cylindrical pores. Molecular Physics. 2015; 114(16-17): 2328-2336. doi: 10.1080/00268976.2015.1090637
62. Marry V, Dufrêche J F, Jardat M, et al. Equilibrium and electrokinetic phenomena in charged porous media from microscopic and mesoscopic models: electro-osmosis in montmorillonite. Molecular Physics. 2003; 101(20): 3111-3119. doi: 10.1080/00268970310001626432
63. Panwar AS, Kumar S. Brownian dynamics simulations of polymer stretching and transport in a complex electroosmotic flow. The Journal of Chemical Physics. 2003; 118(2): 925-936. doi: 10.1063/1.1523912
64. Duong-Hong D, Wang JS, Liu GR, et al. Dissipative particle dynamics simulations of electroosmotic flow in nano-fluidic devices. Microfluidics and Nanofluidics. 2007; 4(3): 219-225. doi: 10.1007/s10404-007-0170-7
65. Moshfegh A, Jabbarzadeh A. Fully explicit dissipative particle dynamics simulation of electroosmotic flow in nanochannels. Microfluidics and Nanofluidics. 2016; 20(4). doi: 10.1007/s10404-016-1733-2
66. Smiatek J, Schmid F. Mesoscopic simulations of electroosmotic flow and electrophoresis in nanochannels. Computer Physics Communications. 2011; 182(9): 1941-1944. doi: 10.1016/j.cpc.2010.11.021